



CERN-PH-EP-2012-001
28 May 2012

**Neutral pion and η meson production
in proton-proton collisions at $\sqrt{s} = 0.9$ TeV and $\sqrt{s} = 7$ TeV**

ALICE Collaboration*

Abstract

The first measurements of the invariant differential cross sections of inclusive π^0 and η meson production at mid-rapidity in proton-proton collisions at $\sqrt{s} = 0.9$ TeV and $\sqrt{s} = 7$ TeV are reported. The π^0 measurement covers the ranges $0.4 < p_t < 7$ GeV/ c and $0.3 < p_t < 25$ GeV/ c for these two energies, respectively. The production of η mesons was measured at $\sqrt{s} = 7$ TeV in the range $0.4 < p_t < 15$ GeV/ c . Next-to-Leading Order perturbative QCD calculations, which are consistent with the π^0 spectrum at $\sqrt{s} = 0.9$ TeV, overestimate those of π^0 and η mesons at $\sqrt{s} = 7$ TeV, but agree with the measured η/π^0 ratio at $\sqrt{s} = 7$ TeV.

arXiv:1205.5724v2 [hep-ex] 5 Apr 2017

*See Appendix A for the list of collaboration members

1 Introduction

Hadron production measurements in proton-proton collisions at the Large Hadron Collider (LHC) [1] energies open a new, previously unexplored domain in particle physics, which allows validation of the predictive power of Quantum Chromo Dynamics (QCD) [2]. A quantitative description of hard processes is provided by perturbative QCD (pQCD) supplemented with parton distribution functions (PDF) $f(x)$ and fragmentation functions (FF) $D(z)$, where x is the fraction of the proton longitudinal momentum carried by a parton and z is the ratio of the observed hadron momentum to the final-state parton momentum. Due to the higher collision energy at the LHC, the PDF and FF can be probed at lower values of x and z , respectively, than in previous experiments. Such measurements can provide further constraints on these functions, which are crucial for pQCD predictions for LHC energies. Furthermore, while pion production at the Relativistic Heavy Ion Collider (RHIC) [3] is considered to be dominated by gluon fragmentation only for $p_t < 5 - 8$ GeV/ c [4, 5], at LHC energies it should remain dominant for $p_t < 100$ GeV/ c [6, 7]. Theoretical estimates [6] suggest that the fraction of pions originating from gluon fragmentation remains above 75 % in the p_t range up to 30 GeV/ c . Here, the measurement of the π^0 production cross section at LHC energies provides constraints on the gluon to pion fragmentation [8] in a new energy regime. In addition, the strange quark content of the η meson makes the comparison to pQCD relevant for possible differences of fragmentation functions with and without strange quarks [9]. Furthermore, the precise measurement of π^0 and η meson spectra over a large p_t range is a prerequisite for understanding the decay photon (electron) background for a direct photon (charm and beauty) measurement. Finally, a significant fraction of hadrons at low p_t is produced in pp collisions via soft parton interactions, which cannot be well described within the framework of pQCD. In this kinematic region commonly used event generators like PYTHIA [10] or PHOJET [11] have to resort to phenomenological models tuned to available experimental data delivered by lower-energy colliders like Sp \bar{p} S, RHIC, and Tevatron [12], to adequately describe hadron production. The large increase in center-of-mass energy at the LHC provides the possibility for a stringent test of the extrapolations based on these models.

This paper presents the first measurement of neutral pion and η meson production in proton-proton collisions at center-of-mass energies of $\sqrt{s} = 0.9$ TeV and 7 TeV in a wide p_t range with the ALICE detector [13]. The paper is organized as follows: description of the subdetectors used for these measurements, followed by the details about the data sample, as well as about event selection and photon identification, is given in section 2. Section 3 describes the algorithms of neutral meson extraction, methods of production spectra measurement, and shows the systematic uncertainty estimation. Results and their comparison with pQCD calculations are given in section 4.

2 Detector description and event selection

Neutral pions and η mesons are measured in ALICE via the two-photon decay channel. The photons are detected with two methods in two independent subsystems, with the Photon Spectrometer (PHOS) [14] and with the photon conversion method (PCM) in the central tracking system employing the Inner Tracking System (ITS) [15] and the Time Projection Chamber (TPC) [16]. The latter reconstructs and identifies photons converted to e^+e^- pairs in the material of the inner detectors. The simultaneous measurements with both methods with completely different systematic uncertainties and with momentum resolutions having opposite dependence on momentum provide a consistency check of the final result.

The PHOS detector consists at present of three modules installed at a distance of 4.60 m from the interaction point. PHOS covers the acceptance of $260^\circ < \varphi < 320^\circ$ in azimuthal angle and $|\eta| < 0.13$ in pseudorapidity. Each module has 3584 detection channels in a matrix of 64×56 cells. Each detection channel consists of a lead tungstate, PbWO_4 , crystal of 2.2×2.2 cm² cross section and 18 cm length, coupled to an avalanche photo diode and a low-noise charge-sensitive preamplifier. PHOS operates at a temperature of -25 °C at which the light yield of the PbWO_4 crystal is increased by about a factor 3

compared to room temperature. PHOS was calibrated in-situ by equalizing mean deposited energies in each channel using events with pp collisions.

The Inner Tracking System (ITS) [13] consists of six layers equipped with Silicon Pixel Detectors (SPD) positioned at a radial distance of 3.9 cm and 7.6 cm, Silicon Drift Detectors (SDD) at 15.0 cm and 23.9 cm, and Silicon Strip Detectors (SSD) at 38.0 cm and 43.0 cm. The two innermost layers cover a pseudorapidity range of $|\eta| < 2$ and $|\eta| < 1.4$, respectively.

The Time Projection Chamber (TPC) [16] is a large (85 m^3) cylindrical drift detector filled with a Ne/CO₂/N₂ (85.7/9.5/4.8%) gas mixture. It is the main tracking system of the Central Barrel. For the maximum track length of 159 clusters it covers a pseudorapidity range of $|\eta| < 0.9$ over the full azimuthal angle. In addition, it provides particle identification via the measurement of the specific ionisation energy loss (dE/dx) with a resolution of 5.5% [16]. The ITS and the TPC are aligned with respect to each other to the level of few hundred μm using cosmic-ray and proton-proton collision data [15].

The event selection was performed with the VZERO detector [17] in addition to the SPD. The VZERO is a forward scintillator hodoscope with two segmented counters located at 3.3 m and -0.9 m from the interaction point. They cover the pseudorapidity ranges $2.8 < \eta < 5.1$ and $-3.7 < \eta < -1.7$, respectively.

The proton-proton collision data used in this analysis were collected by the ALICE experiment in 2010 with the minimum bias trigger MB_{OR} [18]. This trigger required the crossing of two filled bunches and a signal in at least one of the two SPD pixel layers or in one of the VZERO counters. An offline selection based on time and amplitude signals of the VZERO detectors and the SPD was applied to reject beam-induced and noise background [18]. Pileup collision events were identified imposing a criterion based on multiple primary vertices reconstructed with the SPD detector, and removed from the further analysis. The cross sections for the MB_{OR} trigger have been calculated from other measured cross sections at the same energies with appropriate scaling factors. At $\sqrt{s} = 7$ TeV the cross section for the coincidence between signals in the two VZERO detectors, σ_{MBAND} , was measured in a Van-der-Meer scan [19], and the relative factor $\sigma_{\text{MBAND}}/\sigma_{\text{MBOR}} = 0.873$ with negligible error as obtained from data was used. At $\sqrt{s} = 0.9$ TeV the cross section σ_{MBOR} has been calculated from the inelastic cross section measured in $p\bar{p}$ collisions at $\sqrt{s} = 0.9$ TeV [20] and relative factor $\sigma_{\text{MBOR}}/\sigma_{\text{inel}} = 0.91_{-0.01}^{+0.03}$ estimated from Monte Carlo simulations [19].

Table 1 shows the values of the cross section obtained at both energies as well as the integrated luminosity of the total data samples used. In the photon conversion analysis, only events with a reconstructed vertex ($\sim 90\%$ of the total) are inspected, and those events with a longitudinal distance (i.e. along the beam direction) between the position of the primary vertex and the geometrical center of the apparatus larger than 10 cm are discarded. The analysis using PHOS as well as Monte Carlo simulations show that the number of π^0 s in events without a reconstructed vertex is below 1% of the total number of π^0 s.

$\sqrt{s}(\text{TeV})$	$\sigma_{\text{MBOR}} (\text{mb})$	$\sigma_{pp}^{\text{INEL}} (\text{mb})$	
0.9	$47.8_{-1.9}^{+2.4}(\text{syst})$	$52.5 \pm 2(\text{syst})$	
7	$62.2 \pm 2.2(\text{syst})$	$73.2_{-4.6}^{+2.0} \pm 2.6^{\text{lumi}}$	
$\sqrt{s}(\text{TeV})$	$\mathcal{L} (\text{nb}^{-1})$		
	PCM	PHOS π^0	PHOS η
0.9	0.14	0.14	
7	5.6	4.0	5.7

Table 1: Cross sections of the reactions and integrated luminosities of the measured data samples for the two beam energies (top), and luminosities used in the different analyses for the 7 TeV data (bottom).

To maximize the pion reconstruction efficiency in PHOS, only relatively loose cuts on the clusters (group of crystals with deposited energy and common edges) were used: the cluster energy was required to be above the minimum ionizing energy $E_{\text{cluster}} > 0.3$ GeV and the minimum number of crystals in a cluster was three to reduce the contribution of non-photon clusters.

Candidate track pairs for photon conversions were reconstructed using a secondary vertex (V0) finding algorithm [21]. In order to select photons among all secondary vertices (mainly γ , K_S^0 , Λ and $\bar{\Lambda}$), electron selection and pion rejection cuts were applied. The main particle identification (PID) selection used the specific energy loss in the TPC (dE/dx). The measured dE/dx of electrons was required to lie in the interval $[-4\sigma_{dE/dx}, +5\sigma_{dE/dx}]$ around the expected value. In addition, pion contamination was further reduced by a cut of 2σ above the nominal pion dE/dx in the momentum range of 0.25 GeV/c to 3.5 GeV/c and a cut of 0.5σ at higher momenta. For the γ reconstruction constraints on the reconstructed photon mass and on the opening angle between the reconstructed photon momentum vector and the vector joining the collision vertex and the conversion point were applied. These constraints were implemented as a cut on the $\chi^2(\gamma)$ defined using a reconstruction package for fitting decay particles [22]. The photon measurement contains information on the direction which allows to reduce the contamination from secondary neutral pions. With the conversion method a precise γ -ray tomograph of the ALICE experiment has been obtained [23]. The integrated material budget for $r < 180$ cm and $|\eta| < 0.9$ is $11.4 \pm 0.5\%$ X_0 as extracted from detailed comparisons between the measured thickness and its implementation in Monte Carlo simulations based on the GEANT 3.21 package using the same simulation runs for the material studies as for the π^0 measurement. Photon pairs with an opening angle larger than 5 mrad were selected for the meson analysis.

3 Neutral meson reconstruction

Neutral pions and η mesons are reconstructed as excess yields, visible as peaks at their respective rest mass, above the combinatorial background in the two-photon invariant mass spectrum. Invariant mass spectra demonstrating the π^0 and η mesons peak in some selected p_t slices are shown in Fig.1 by the histogram. The background is determined by mixing photon pairs from different events and is normalized

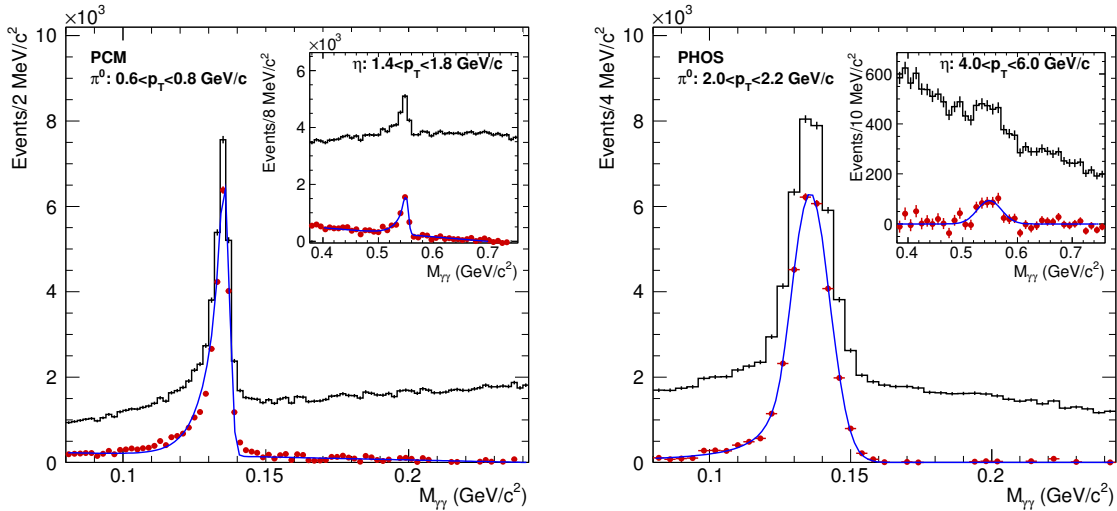


Fig. 1: Invariant mass spectra in selected p_t slices in PCM (left) and PHOS (right) in the π^0 and η meson mass regions. The histogram and the bullets show the data before and after background subtraction, respectively. The curve is a fit to the invariant mass spectrum after background subtraction.

to the same event background at the right side of the meson peaks. A residual correlated background is further subtracted using a linear or second order polynomial fit. The invariant mass spectrum after

background subtraction, depicted by bullets in Fig.1, was fitted to obtain the π^0 and η peak parameters (a curve). The number of reconstructed π^0 s (η s) is obtained in each p_t bin by integrating the background subtracted peak within 3 standard deviations around the mean value of the π^0 (η) peak position in the case of PHOS. In the PCM measurement the integration windows were chosen to be asymmetric ($m_{\pi^0}-0.035$ GeV/ c^2 , $m_{\pi^0}+0.010$ GeV/ c^2) and ($m_{\eta}-0.047$ GeV/ c^2 , $m_{\eta}+0.023$ GeV/ c^2) to take into account the left side tail of the meson peaks due to bremsstrahlung. For the same reason in the case of PCM the full width at half maximum (FWHM) instead of the Gaussian width of the peak was used. We vary the normalization and integration windows to estimate the related systematic uncertainties. The peak position and width from the two analyses compared to Monte Carlo simulations are shown in Fig. 2 as a function of p_t .

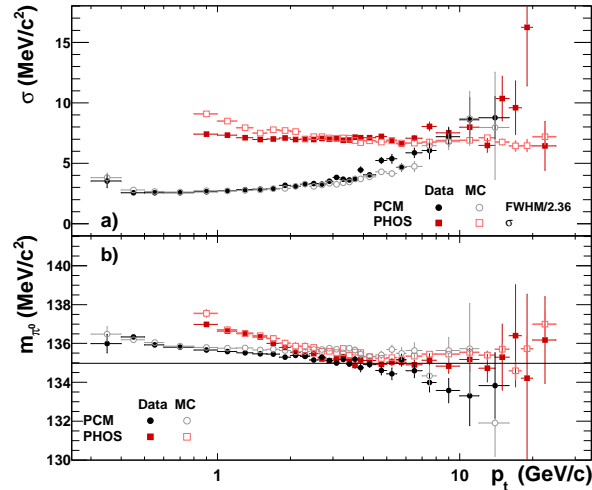


Fig. 2: Reconstructed π^0 peak width (a) and position (b) as a function of p_t in pp collisions at $\sqrt{s} = 7$ TeV in PHOS and in the photon conversion method (PCM) compared to Monte Carlo simulations. The horizontal line in (b) indicates the nominal π^0 mass.

The reconstruction efficiency ε and acceptance A are calculated in Monte Carlo simulations tuned to reproduce the detector response. In the PHOS case, the tuning included a 4.5% energy non-linearity observed in real data at $E < 1$ GeV and not reproduced by the GEANT simulations and an additional 6% channel-by-channel decalibration. In the PCM case, an additional smearing in each momentum component given by $\sigma = \sqrt{\sigma_0^2 + \sigma_1^2 \cdot p^2}$ with $\sigma_0 = 0.011$ GeV/ c and $\sigma_1 = 0.007$ was necessary to reproduce the measured width of the π^0 peak. PYTHIA [10] and PHOJET [11] event generators and single particle simulations were used as input. The small photon conversion probability of about 8.5%, compensated by the large TPC acceptance, translates into $\varepsilon \cdot A$ of about 2×10^{-3} at $p_t > 1$ GeV/ c and decreases at lower p_t due to the decrease of the efficiency of soft electron reconstruction and conversion probability. In the PHOS case, the acceptance A is zero for $p_t < 0.4$ GeV/ c , $\varepsilon \cdot A$ increases with p_t and saturates at about 2.0×10^{-2} at $p_t > 15$ GeV/ c . At high $p_t > 25$ GeV/ c the efficiency decreases due to cluster merging.

The invariant differential cross section of π^0 and η meson production were calculated as

$$E \frac{d^3\sigma}{dp^3} = \frac{1}{2\pi} \frac{\sigma_{\text{MBOR}}}{N_{\text{events}}} \frac{1}{p_t} \frac{1}{\varepsilon A Br} \frac{N^{\pi^0(\eta)}}{\Delta y \Delta p_t}, \quad (1)$$

where σ_{MBOR} is the interaction cross section for the MBOR trigger for pp collisions at $\sqrt{s} = 0.9$ TeV or $\sqrt{s} = 7$ TeV, N_{events} is the number of MBOR events, p_t is the transverse momentum within the bin to which the cross section has been assigned after the correction for the finite bin width Δp_t (see below), Br is the branching ratio of the π^0 (η) meson to the two γ decay channel and $N^{\pi^0(\eta)}$ is the number of reconstructed π^0 (η) mesons in a given Δy and Δp_t bin. Finally, the invariant cross sections were

corrected for the finite p_t bin width following the prescription in [24], keeping the y values equal to the bin averages and calculating the p_t position at which the differential cross section coincides with the bin average. The Tsallis fit (see below) was used for the correction. Secondary π^0 's from weak decays or hadronic interactions in the detector material are subtracted using Monte Carlo simulations. The contribution from K_S^0 decays is scaled using the measured K_S^0 spectrum at $\sqrt{s} = 0.9$ TeV [30] or the charged kaon spectra at $\sqrt{s} = 7$ TeV [31]. The measured π^0 and η meson spectra at the center-of-mass energy of $\sqrt{s} = 7$ TeV cover a p_t range from 0.3 to 25 GeV/ c and from 0.4 to 15 GeV/ c , respectively; the π^0 spectra at $\sqrt{s} = 0.9$ TeV cover a p_t range from 0.4 to 7 GeV/ c .

	PHOS	
	$p_t = 1.1$ GeV/ c	$p_t = 7.5$ GeV/ c
Yield extr.	± 2.1	± 2.5
Non-linearity	± 9.0	± 1.5
Conversion	± 3.5	± 3.5
Absolute energy scale	± 0.7	± 1.0
Acceptance	± 1.0	± 1.0
Calibration and alignment	± 7.0	± 3.0
Pileup	± 0.8	± 0.8
Total	$\pm 12.5\%$	$\pm 6.0\%$
	PCM	
	$p_t=1.1$ GeV/ c	$p_t=7.5$ GeV/ c
Material Budget	± 9.0	± 9.0
Yield extraction	± 0.6	± 4.9
PID	± 0.1	± 5.4
$\chi^2(\gamma)$	± 0.3	± 6.2
Reconstruction ϵ	± 1.9	± 4.9
Total	$\pm 9.2\%$	$\pm 14.0\%$

Table 2: Summary of the relative systematic errors for the PHOS and the PCM analyses.

A summary of the systematic uncertainties is shown in Table 2 for two different p_t values. In PHOS, the significant source of systematic errors both at low and high p_t is the raw yield extraction. It was estimated by varying the fitting range and the assumption about the shape of the background around the peak. The uncertainty related to the non-linearity of PHOS which dominates at low p_t was estimated by introducing different non-linearities into the MC simulations under the condition that the simulated p_t -dependence of the π^0 peak position and peak width is still consistent with data. The uncertainties on the calibration and alignment were estimated in Monte Carlo simulations by varying the calibration parameters and the relative module positions within the expected tolerances. The uncertainty related to the pileup event rejection was evaluated in data by estimating the fraction of unidentified pileup events by extrapolating the distance and the number of contributing tracks of found pileup vertices to zero. The uncertainty of the conversion probability was estimated comparing measurements without magnetic field to the standard measurements with magnetic field. In the measurements with converted photons, the main sources of systematic errors are the knowledge of the material budget (dominant at low p_t), raw yield extraction, PID, the photon χ^2 cut and reconstruction efficiency. The contribution from the raw yield extraction was estimated by changing the normalization range, the integration window, and the combinatorial background evaluation. The PID, photon $\chi^2(\gamma)$ cut and reconstruction efficiency was estimated by evaluating stability of the results after changing the cut values.

Meson	\sqrt{s} TeV	A	C (MeV/c ²)	n
π^0	0.9	1.5 ± 0.3	132 ± 15	7.8 ± 0.5
π^0	7	2.40 ± 0.15	139 ± 4	6.88 ± 0.07
η	7	0.21 ± 0.03	229 ± 21	7.0 ± 0.5

Table 3: Fit parameters of the Tsallis parametrisation (2) to the combined invariant production yields of π^0 and η mesons for inelastic events. The uncertainty on the parameter A due to the spectra normalization of $^{+3.2}_{-1.1}\%$ and $^{+7.0}_{-3.5}\%$ at $\sqrt{s} = 900$ GeV, and 7 TeV respectively, is not included.

4 Results and comparison with pQCD

The combined spectrum is calculated as a weighted average using statistical and systematic errors of the individual analyses [25]. The combined production cross sections are shown in Fig. 3 a). The combined spectra including statistical and systematic errors are fitted with the Tsallis function [26]

$$E \frac{d^3\sigma}{dp^3} = \frac{\sigma_{pp}^{\text{INEL}}}{2\pi} A \frac{c \cdot (n-1)(n-2)}{nC [nC + m(n-2)]} \left(1 + \frac{m_t - m}{nC}\right)^{-n}, \quad (2)$$

where the fit parameters are A, C and n, σ_{pp} is the proton-proton inelastic cross section, m is the meson rest mass and $m_t = \sqrt{m^2 + p_t^2}$ is the transverse mass. The fit parameters are shown in Table 3. The property of the Tsallis function (2) is such that the parameter A is equal to the integral of this function over p_t from 0 to infinity, $A = dN/dy$, and thus can be used as an estimation of the total yield at $y = 0$ per inelastic pp collision. The additional uncertainty on the parameter A due to the spectra normalization of $^{+3.2}_{-1.1}\%$ and $^{+7.0}_{-3.5}\%$ at $\sqrt{s} = 900$ GeV, and 7 TeV respectively, is not included. The found parameters of the Tsallis function for π^0 production spectrum in pp collisions at $\sqrt{s} = 900$ GeV are in agreement with those for the $\pi^+ + \pi^-$ spectra measured by the ALICE collaboration at the same energy [27].

The ratio of the data points of the two methods to the combined fit, shown in Fig. 4, illustrates the consistency between the two measurements.

We compare our results with Next-to-Leading Order (NLO) pQCD calculations using the PDF CTEQ6M5 and DSS π^0 [8], BKK π^0 [29] and AESSS η [9] NLO fragmentation functions, see Fig. 3 a). The data and NLO predictions are compared via a ratio with the fit to the measured cross section. This is shown in the bottom panels (b), (c) and (d) in Fig. 3. In the NLO calculations the factorization, renormalization and fragmentation scales are chosen to have the same value given by μ . The uncertainty in the inelastic pp cross section is represented by the full boxes at unity. At $\sqrt{s} = 0.9$ TeV the NLO calculations at $\mu = 1 p_t$ describe the measured π^0 data well, while at $\sqrt{s} = 7$ TeV the higher scale ($\mu = 2 p_t$) and a different set of fragmentation functions are required for a description of the data. However, the latter parameter set does not provide a good description of the low energy data. In any case, the NLO pQCD calculations show a harder slope compared to the measured results. Using the INCNLO program [28], we tested different parton distribution functions (CTEQ5M, CTEQ6M, MRS99) and different fragmentation functions (BKK, KKP, DSS) and found a similar result: pQCD predicts harder slopes, and variation of PDFs and FFs does not change the shape, but results mainly in the variation of the absolute cross section. A similar trend is observed for the η meson (a higher scale $\mu = 2 p_t$ is required), although the discrepancy is less significant due to the larger error bars and smaller p_t reach.

The ratio η/π^0 is shown in Fig. 5. It has the advantage that systematic uncertainties in the measurement partially cancel. This is also the case for the NLO pQCD calculation, where in particular the influence of the PDF is reduced in the ratio. Here, predictions that failed to reproduce the measured π^0 and η cross section are able to reproduce the η/π^0 ratio.

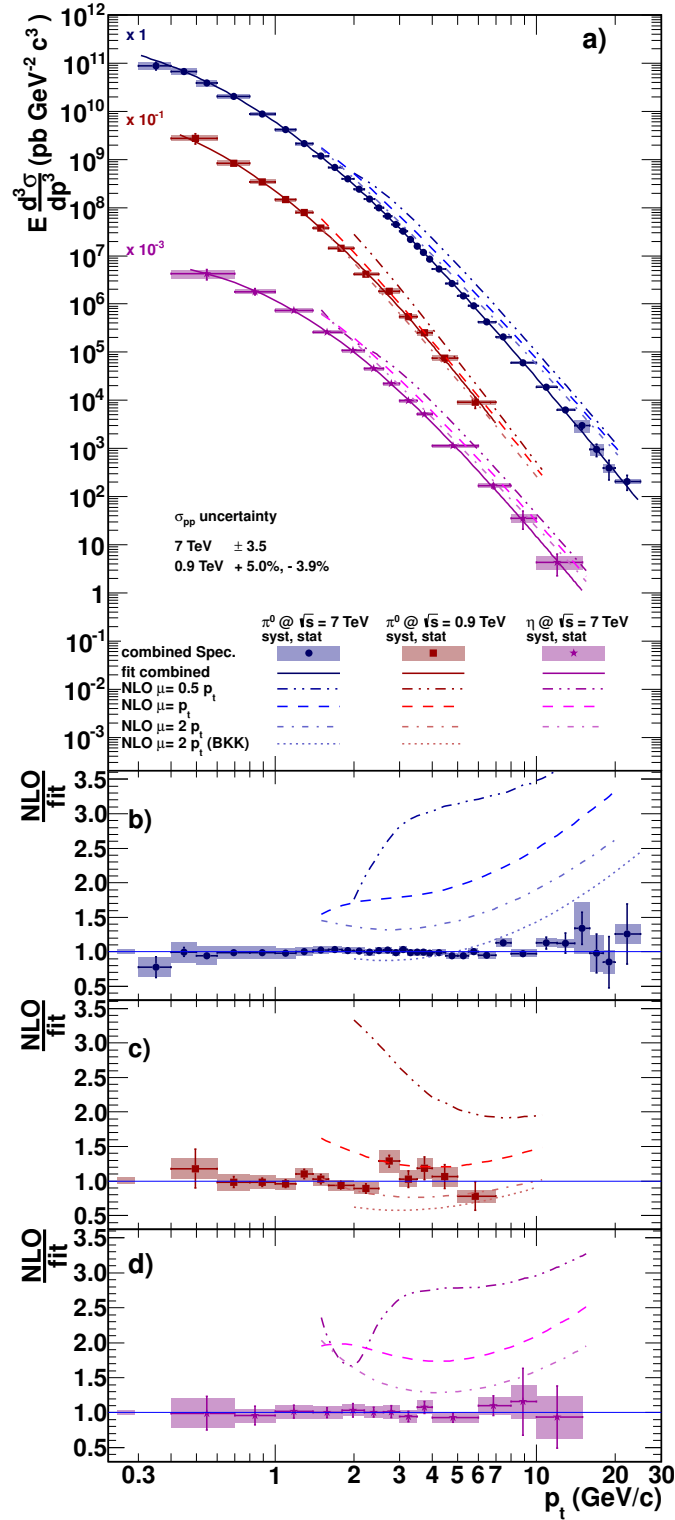


Fig. 3: a) Differential invariant cross section of π^0 production in pp collisions at $\sqrt{s} = 7$ TeV (circles) and 0.9 TeV (squares) and of η meson production at $\sqrt{s} = 7$ TeV (stars). The lines and the boxes represent the statistical and systematic error of the combined measurement respectively. The uncertainty on the pp cross section is not included. NLO pQCD calculations using the CTEQ6M5 PDF and the DSS (AESS for η mesons) FF for three scales $\mu = 0.5p_t, 1p_t$ and $2p_t$ are shown. Dotted lines in panels b) and c) correspond to the ratios using the BKK FF. Ratio of the NLO calculations to the data parametrisations are shown in panels b), c) and d). The full boxes represent the uncertainty on the pp cross sections.

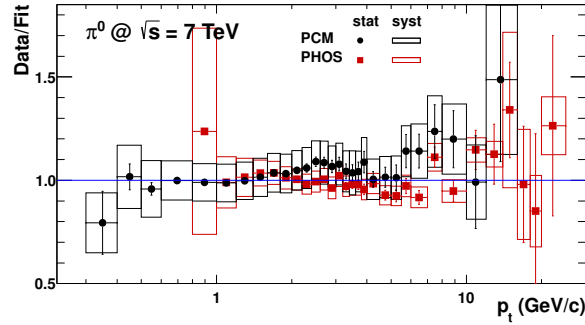


Fig. 4: Ratio of the two independent π^0 meson measurements to the fit of the combined normalized invariant production cross section of π^0 mesons in pp collisions at $\sqrt{s} = 7$ TeV.

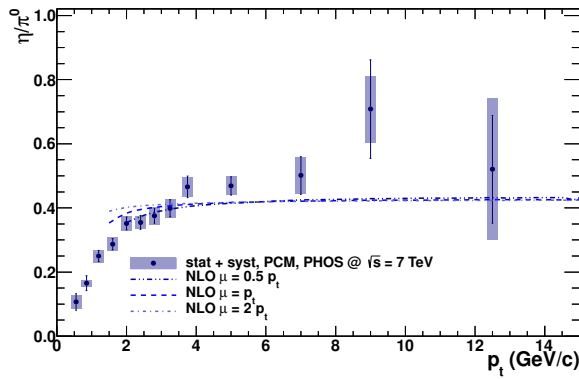


Fig. 5: η/π^0 ratio measured in pp collisions at $\sqrt{s} = 7$ TeV compared to NLO pQCD predictions.

5 Conclusion

In summary, the invariant differential cross sections for inclusive π^0 production in pp collisions at $\sqrt{s} = 7$ TeV and 0.9 TeV and for η meson production at 7 TeV have been measured in a wide p_t range taking advantage of two independent methods available in the ALICE experiment at the LHC. NLO pQCD calculations cannot provide a consistent description of measured data at both beam energies. State-of-the-art calculations describe the data at 0.9 TeV and 0.2 TeV [32], however this is not the case at 7 TeV, where the calculations overestimate the cross sections and exhibit a different slope compared to the data. Thus, this measurement provides an important input for the tuning of pQCD calculations and represents crucial reference data for the measurement of the nuclear modification factor R_{AA} of the π^0 production in heavy-ion collisions at the LHC. Furthermore, the NLO predictions for the η mesons using the newest fragmentation functions require a value $\mu = 2p_t$ in order to get closer to the experimental results.

6 Acknowledgments

The ALICE collaboration would like to thank all its engineers and technicians for their invaluable contributions to the construction of the experiment and the CERN accelerator teams for the outstanding performance of the LHC complex.

The ALICE collaboration acknowledges the following funding agencies for their support in building and running the ALICE detector:

Calouste Gulbenkian Foundation from Lisbon and Swiss Fonds Kidagan, Armenia;

Conselho Nacional de Desenvolvimento Científico e Tecnológico (CNPq), Financiadora de Estudos e Projetos (FINEP), Fundação de Amparo à Pesquisa do Estado de São Paulo (FAPESP);

National Natural Science Foundation of China (NSFC), the Chinese Ministry of Education (CMOE) and the Ministry of Science and Technology of China (MSTC);

Ministry of Education and Youth of the Czech Republic;
Danish Natural Science Research Council, the Carlsberg Foundation and the Danish National Research Foundation;
The European Research Council under the European Community's Seventh Framework Programme;
Helsinki Institute of Physics and the Academy of Finland;
French CNRS-IN2P3, the 'Region Pays de Loire', 'Region Alsace', 'Region Auvergne' and CEA, France;
German BMBF and the Helmholtz Association;
General Secretariat for Research and Technology, Ministry of Development, Greece;
Hungarian OTKA and National Office for Research and Technology (NKTH);
Department of Atomic Energy and Department of Science and Technology of the Government of India;
Istituto Nazionale di Fisica Nucleare (INFN) of Italy;
MEXT Grant-in-Aid for Specially Promoted Research, Japan;
Joint Institute for Nuclear Research, Dubna;
National Research Foundation of Korea (NRF);
CONACYT, DGAPA, México, ALFA-EC and the HELEN Program (High-Energy physics Latin-American-European Network);
Stichting voor Fundamenteel Onderzoek der Materie (FOM) and the Nederlandse Organisatie voor Wetenschappelijk Onderzoek (NWO), Netherlands;
Research Council of Norway (NFR);
Polish Ministry of Science and Higher Education;
National Authority for Scientific Research - NASR (Autoritatea Națională pentru Cercetare Științifică - ANCS);
Federal Agency of Science of the Ministry of Education and Science of Russian Federation, International Science and Technology Center, Russian Academy of Sciences, Russian Federal Agency of Atomic Energy, Russian Federal Agency for Science and Innovations and CERN-INTAS;
Ministry of Education of Slovakia;
Department of Science and Technology, South Africa;
CIEMAT, EELA, Ministerio de Educación y Ciencia of Spain, Xunta de Galicia (Consellería de Educación), CEADEN, Cubaenergía, Cuba, and IAEA (International Atomic Energy Agency);
Swedish Research Council (VR) and Knut & Alice Wallenberg Foundation (KAW);
Ukraine Ministry of Education and Science;
United Kingdom Science and Technology Facilities Council (STFC);
The United States Department of Energy, the United States National Science Foundation, the State of Texas, and the State of Ohio.

This job was supported partially by the grant RFBR 10-02-91052. We would like to thank W. Vogelsang for providing the NLO pQCD calculations used in this paper.

References

- [1] L. Evans, (ed.), P. Bryant, (ed.), JINST **3**, S08001 (2008).
- [2] D. J. Gross, F. Wilczek, Phys. Rev. **D8**, 3633-3652 (1973).
- [3] P. J. Reardon, Nucl. Phys. **A478**, 861C-873C (1988).
- [4] R. Vogt, "Ultrarelativistic heavy-ion collisions," *Amsterdam, Netherlands: Elsevier (2007) 477 p*
- [5] A. Adare *et al.* [PHENIX Collaboration], Phys. Rev. D **83** (2011) 032001 [arXiv:1009.6224 [hep-ex]].
- [6] R. Sassot, P. Zurita, M. Stratmann, Phys. Rev. **D82**, 074011 (2010). [arXiv:1008.0540 [hep-ph]].
- [7] P. Chiappetta, M. Greco, J. P. Guillet, S. Rolli and M. Werlen, Nucl. Phys. B **412** (1994) 3 [arXiv:hep-ph/9301254].

- [8] D. de Florian, R. Sassot, M. Stratmann, Phys. Rev. **D75**, 114010 (2007). [hep-ph/0703242 [HEP-PH]].
- [9] C. A. Aidala, F. Ellinghaus, R. Sassot, J. P. Seele, M. Stratmann, Phys. Rev. **D83**, 034002 (2011). [arXiv:1009.6145 [hep-ph]].
- [10] T. Sjöstrand, S. Mrenna, P. Z. Skands, JHEP **0605**, 026 (2006). [hep-ph/0603175].
- [11] R. Engel, J. Ranft, S. Roesler, Phys. Rev. **D52**, 1459-1468 (1995). [hep-ph/9502319].
- [12] T. Aaltonen *et al.* [CDF Collaboration], Phys. Rev. **D79**, 112005 (2009). [arXiv:0904.1098 [hep-ex]].
- [13] K. Aamodt *et al.* [ALICE Collaboration], JINST **3**, S08002 (2008).
- [14] G. Dellacasa *et al.* [ALICE Collaboration], Photon Spectrometer PHOS, Technical Design Report. CERN/LHCC 99-4, 5 March 1999.
- [15] K. Aamodt *et al.* [ALICE Collaboration], JINST **5**, P03003 (2010). [arXiv:1001.0502 [physics.ins-det]].
- [16] J. Alme, Y. Andres, H. Appelshauser, S. Bablok, N. Bialas, R. Bolgen, U. Bonnes, R. Bramm *et al.*, Nucl. Instrum. Meth. **A622**, 316-367 (2010). [arXiv:1001.1950 [physics.ins-det]].
- [17] P. Cortese *et al.* [ALICE collaboration], ALICE forward detectors: FMD, TO and VO: Technical Design Report, CERN-LHCC-2004-025, <http://cdsweb.cern.ch/record/781854>.
- [18] K. Aamodt *et al.* [ALICE Collaboration], Eur. Phys. J. **C68**, 345-354 (2010). [arXiv:1004.3514 [hep-ex]].
- [19] K. Aamodt, *et al.* [ALICE collaboration], to be published.
- [20] G. J. Alner *et al.* [UA5 Collaboration], Z. Phys. C **32** (1986) 153.
- [21] G. Alessandro, (Ed.) *et al.* [ALICE Collaboration], J. Phys. G **G32**, 1295-2040 (2006).
- [22] "Reconstruction of decay particles based on the Kalman filter", S. Gorbunov and I. Kisel, CBM-SOFT-note-2007-003, GSI, Darmstadt (2007).
- [23] K. Koch [ALICE Collaboration], Nucl. Phys. A **855** 281-284 (2011); F. Bock, Bachelor Thesis, University of Heidelberg (2010).
- [24] G. D. Lafferty, T. R. Wyatt, Nucl. Instrum. Meth. **A355**, 541-547 (1995).
- [25] K. Nakamura *et al.* [Particle Data Group Collaboration], J. Phys. **G37**, 075021 (2010).
- [26] C. Tsallis, J. Statist. Phys. **52**, 479-487 (1988).
- [27] K. Aamodt *et al.* [ALICE Collaboration], Eur. Phys. J. C **71** (2011) 1655 [arXiv:1101.4110 [hep-ex]].
- [28] P. Aurenche, M. Fontannaz, J. P. Guillet, B. A. Kniehl, M. Werlen, Eur. Phys. J. **C13**, 347-355 (2000). [arXiv:hep-ph/9910252 [hep-ph]].
- [29] J. Binnewies, B. A. Kniehl and G. Kramer, Z. Phys. C **65** (1995) 471 [arXiv:hep-ph/9407347].
- [30] K. Aamodt *et al.* [ALICE Collaboration], Eur. Phys. J. C **71** (2011) 1594 [arXiv:1012.3257 [hep-ex]].
- [31] M. Floris [ALICE Collaboration], arXiv:1108.3257 [hep-ex].
- [32] A. Adare *et al.* [PHENIX Collaboration], Phys. Rev. D **76** (2007) 051106 [arXiv:0704.3599 [hep-ex]].

A The ALICE Collaboration

B. Abelev⁶⁹, A. Abrahantes Quintana⁶, D. Adamová⁷⁴, A.M. Adare¹²⁰, M.M. Aggarwal⁷⁸, G. Aglieri Rinella³⁰, A.G. Agocs⁶⁰, A. Agostinelli¹⁹, S. Aguilar Salazar⁵⁶, Z. Ahammed¹¹⁶, N. Ahmad¹⁴, A. Ahmad Masoodi¹⁴, S.U. Ahn^{64,37}, A. Akindinov⁴⁶, D. Aleksandrov⁸⁹, B. Alessandro⁹⁵, R. Alfaro Molina⁵⁶, A. Alici^{96,30,9}, A. Alkin², E. Almaráz Aviña⁵⁶, T. Alt³⁶, V. Altini^{28,30}, S. Altinpinar¹⁵, I. Altsybeev¹¹⁷, C. Andrei⁷¹, A. Andronic⁸⁶, V. Anguelov⁸³, C. Anson¹⁶, T. Antičić⁸⁷, F. Antinori¹⁰⁰, P. Antonioli⁹⁶, L. Aphecetche¹⁰², H. Appelshäuser⁵², N. Arbor⁶⁵, S. Arcelli¹⁹, A. Arend⁵², N. Armesto¹³, R. Arnaldi⁹⁵, T. Aronsson¹²⁰, I.C. Arsene⁸⁶, M. Arslanok⁵², A. Asryan¹¹⁷, A. Augustinus³⁰, R. Averbeck⁸⁶, T.C. Awes⁷⁵, J. Äystö³⁸, M.D. Azmi¹⁴, M. Bach³⁶, A. Badalá⁹⁷, Y.W. Baek^{64,37}, R. Bailhache⁵², R. Bala⁹⁵, R. Baldini Ferroli⁹, A. Baldisseri¹², A. Baldit⁶⁴, F. Baltasar Dos Santos Pedrosa³⁰, J. Bán⁴⁷, R.C. Baral⁴⁸, R. Barbera²⁴, F. Barile²⁸, G.G. Barnaföldi⁶⁰, L.S. Barnby⁹¹, V. Barret⁶⁴, J. Bartke¹⁰⁴, M. Basile¹⁹, N. Bastid⁶⁴, B. Bathen⁵⁴, G. Batigne¹⁰², B. Batyunya⁵⁹, C. Baumann⁵², I.G. Bearden⁷², H. Beck⁵², I. Belikov⁵⁸, F. Bellini¹⁹, R. Bellwied¹¹⁰, E. Belmont-Moreno⁵⁶, S. Beole²⁶, I. Berceau⁷¹, A. Bercuci⁷¹, Y. Berdnikov⁷⁶, D. Berenyi⁶⁰, C. Bergmann⁵⁴, D. Berzano⁹⁵, L. Betev³⁰, A. Bhasin⁸¹, A.K. Bhati⁷⁸, N. Bianchi⁶⁶, L. Bianchi²⁶, C. Bianchin²², J. Bielčik³⁴, J. Bielčiková⁷⁴, A. Bilandzic⁷³, F. Blanco⁷, F. Blanco¹¹⁰, D. Blau⁸⁹, C. Blume⁵², M. Boccioni³⁰, F. Bock⁸³, N. Bock¹⁶, A. Bogdanov⁷⁰, H. Bøggild⁷², M. Bogolyubsky⁴³, L. Boldizsár⁶⁰, M. Bombara³⁵, J. Book⁵², H. Borel¹², A. Borissov¹¹⁹, C. Bortolin^{22,ii}, S. Bose⁹⁰, F. Bossú^{30,26}, M. Botje⁷³, S. Böttger⁵¹, B. Boyer⁴², P. Braun-Munzinger⁸⁶, M. Bregant¹⁰², T. Breitner⁵¹, M. Broz³³, R. Brun³⁰, E. Bruna^{120,26,95}, G.E. Bruno²⁸, D. Budnikov⁸⁸, H. Buesching⁵², S. Bufalino^{26,95}, K. Bugaiev², O. Busch⁸³, Z. Buthelezi⁸⁰, D. Caffarri²², X. Cai⁴⁰, H. Caines¹²⁰, E. Calvo Villar⁹², P. Camerini²⁰, V. Canoa Roman^{8,1}, G. Cara Romeo⁹⁶, F. Carena³⁰, W. Carena³⁰, N. Carlin Filho¹⁰⁷, F. Carminati³⁰, C.A. Carrillo Montoya³⁰, A. Casanova Díaz⁶⁶, M. Caselle³⁰, J. Castillo Castellanos¹², J.F. Castillo Hernandez⁸⁶, E.A.R. Casula²¹, V. Catanesu⁷¹, C. Cavicchioli³⁰, J. Cepila³⁴, P. Cerello⁹⁵, B. Chang^{38,123}, S. Chapeland³⁰, J.L. Charvet¹², S. Chattopadhyay⁹⁰, S. Chattopadhyay¹¹⁶, M. Chorney⁷⁷, C. Cheshkov^{30,109}, B. Cheynis¹⁰⁹, E. Chiavassa⁹⁵, V. Chibante Barroso³⁰, D.D. Chinellato¹⁰⁸, P. Chochula³⁰, M. Chojnacki⁴⁵, P. Christakoglou^{73,45}, C.H. Christensen⁷², P. Christiansen²⁹, T. Chujo¹¹⁴, S.U. Chung⁸⁵, C. Cicalo⁹³, L. Cifarelli^{19,30}, F. Cindolo⁹⁶, J. Cleymans⁸⁰, F. Coccetti⁹, J.-P. Coffin⁵⁸, F. Colamaria²⁸, D. Colella²⁸, G. Conesa Balbastre⁶⁵, Z. Conesa del Valle^{30,58}, P. Constantin⁸³, G. Contin²⁰, J.G. Contreras⁸, T.M. Cormier¹¹⁹, Y. Corrales Morales²⁶, P. Cortese²⁷, I. Cortés Maldonado¹, M.R. Cosentino^{68,108}, F. Costa³⁰, M.E. Cotallo⁷, E. Crescio⁸, P. Crochet⁶⁴, E. Cruz Alaniz⁵⁶, E. Cuautle⁵⁵, L. Cunqueiro⁶⁶, A. Dainese^{22,100}, H.H. Dalsgaard⁷², A. Danu⁵⁰, I. Das^{90,42}, K. Das⁹⁰, D. Das⁹⁰, A. Dash^{48,108}, S. Dash^{41,95}, S. De¹¹⁶, A. De Azevedo Moregula⁶⁶, G.O.V. de Barros¹⁰⁷, A. De Caro^{25,9}, G. de Cataldo⁹⁴, J. de Cuveland³⁶, A. De Falco²¹, D. De Gruttola²⁵, H. Delagrangé¹⁰², E. Del Castillo Sanchez³⁰, A. Deloff¹⁰¹, V. Demanov⁸⁸, N. De Marco⁹⁵, E. Dénes⁶⁰, S. De Pasquale²⁵, A. Deppman¹⁰⁷, G. D Eraso²⁸, R. de Rooij⁴⁵, D. Di Bari²⁸, T. Dietel⁵⁴, C. Di Giglio²⁸, S. Di Liberto⁹⁹, A. Di Mauro³⁰, P. Di Nezza⁶⁶, R. Diviá³⁰, Ø. Djuvsland¹⁵, A. Dobrin^{119,29}, T. Dobrowolski¹⁰¹, I. Domínguez⁵⁵, B. Dönigus⁸⁶, O. Dordic¹⁸, O. Driga¹⁰², A.K. Dubey¹¹⁶, L. Ducroux¹⁰⁹, P. Dupieux⁶⁴, M.R. Dutta Majumdar¹¹⁶, A.K. Dutta Majumdar⁹⁰, D. Elia⁹⁴, D. Emschermann⁵⁴, H. Engel⁵¹, H.A. Erdal³², B. Espagnon⁴², M. Estienne¹⁰², S. Esumi¹¹⁴, D. Evans⁹¹, G. Eyyubova¹⁸, D. Fabris^{22,100}, J. Faivre⁶⁵, D. Falchieri¹⁹, A. Fantoni⁶⁶, M. Fasel⁸⁶, R. Fearick⁸⁰, A. Fedunov⁵⁹, D. Fehlker¹⁵, L. Feldkamp⁵⁴, D. Felea⁵⁰, G. Feofilov¹¹⁷, A. Fernández Téllez¹, A. Ferretti²⁶, R. Ferretti²⁷, J. Figiel¹⁰⁴, M.A.S. Figueredo¹⁰⁷, S. Filchagin⁸⁸, R. Fini⁹⁴, D. Finogeev⁴⁴, F.M. Fionda²⁸, E.M. Fiore²⁸, M. Floris³⁰, S. Foertsch⁸⁰, P. Foka⁸⁶, S. Fokin⁸⁹, E. Fragiaco⁹⁸, M. Fragiadakis⁷⁹, U. Frankenfeld⁸⁶, U. Fuchs³⁰, C. Furget⁶⁵, M. Fusco Girard²⁵, J.J. Gaardhøje⁷², M. Gagliardi²⁶, A. Gago⁹², M. Gallio²⁶, D.R. Gangadharan¹⁶, P. Ganoti⁷⁵, C. Garabatos⁸⁶, E. Garcia-Solis¹⁰, I. Garishvili⁶⁹, J. Gerhard³⁶, M. Germain¹⁰², C. Geuna¹², A. Gheata³⁰, M. Gheata³⁰, B. Ghidini²⁸, P. Ghosh¹¹⁶, P. Gianotti⁶⁶, M.R. Girard¹¹⁸, P. Giubellino³⁰, E. Gladysz-Dziadus¹⁰⁴, P. Gläsel⁸³, R. Gomez¹⁰⁶, E.G. Ferreira¹³, L.H. González-Trueba⁵⁶, P. González-Zamora⁷, S. Gorbunov³⁶, A. Goswami⁸², S. Gotovac¹⁰³, V. Grabski⁵⁶, L.K. Graczykowski¹¹⁸, R. Grajcarek⁸³, A. Grelli⁴⁵, C. Grigoras³⁰, A. Grigoras³⁰, V. Grigoriev⁷⁰, A. Grigoryan¹²¹, S. Grigoryan⁵⁹, B. Grinyov², N. Grión⁹⁸, P. Gros²⁹, J.F. Grosse-Oetringhaus³⁰, J.-Y. Grossiord¹⁰⁹, R. Grosso³⁰, F. Guber⁴⁴, R. Guernane⁶⁵, C. Guerra Gutierrez⁹², B. Guerzoni¹⁹, M. Guilbaud¹⁰⁹, K. Gulbrandsen⁷², T. Gunji¹¹³, A. Gupta⁸¹, R. Gupta⁸¹, H. Gutbrod⁸⁶, Ø. Haaland¹⁵, C. Hadjidakis⁴², M. Haiduc⁵⁰, H. Hamagaki¹¹³, G. Hamar⁶⁰, B.H. Han¹⁷, L.D. Hanratty⁹¹, A. Hansen⁷², Z. Harmanova³⁵, J.W. Harris¹²⁰, M. Hartig⁵², D. Hasegan⁵⁰, D. Hatzifotiadou⁹⁶, A. Hayrapetyan^{30,121}, S.T. Heckel⁵², M. Heide⁵⁴, H. Helstrup³², A. Herghelegiu⁷¹, G. Herrera Corral⁸, N. Herrmann⁸³, K.F. Hetland³², B. Hicks¹²⁰, P.T. Hille¹²⁰, B. Hippolyte⁵⁸, T. Horaguchi¹¹⁴, Y. Hori¹¹³, P. Hristov³⁰, I. Hřivnáčová⁴², M. Huang¹⁵, S. Huber⁸⁶, T.J. Humanic¹⁶, D.S. Hwang¹⁷, R. Ichou⁶⁴, R. Ilkaev⁸⁸, I. Ilkiv¹⁰¹,

M. Inaba¹¹⁴, E. Incani²¹, P.G. Innocenti³⁰, G.M. Innocenti²⁶, M. Ippolitov⁸⁹, M. Irfan¹⁴, C. Ivan⁸⁶,
 M. Ivanov⁸⁶, V. Ivanov⁷⁶, A. Ivanov¹¹⁷, O. Ivanytskyi², A. Jachořkowski³⁰, P. M. Jacobs⁶⁸, L. Jancurová⁵⁹,
 H.J. Jang⁶³, S. Jangal⁵⁸, R. Janik³³, M.A. Janik¹¹⁸, P.H.S.Y. Jayarathna¹¹⁰, S. Jena⁴¹,
 R.T. Jimenez Bustamante⁵⁵, L. Jirden³⁰, P.G. Jones⁹¹, W. Jung³⁷, H. Jung³⁷, A. Jusko⁹¹, A.B. Kaidalov⁴⁶,
 V. Kakoyan¹²¹, S. Kalcher³⁶, P. Kaliňák⁴⁷, M. Kalisky⁵⁴, T. Kalliokoski³⁸, A. Kalweit⁵³, K. Kanaki¹⁵,
 J.H. Kang¹²³, V. Kaplin⁷⁰, A. Karasu Uysal^{30,122}, O. Karavichev⁴⁴, T. Karavicheva⁴⁴, E. Karpechev⁴⁴,
 A. Kazantsev⁸⁹, U. Kebschull^{62,51}, R. Keidel¹²⁴, P. Khan⁹⁰, M.M. Khan¹⁴, S.A. Khan¹¹⁶, A. Khanzadeev⁷⁶,
 Y. Kharlov⁴³, B. Kileng³², J.H. Kim¹⁷, D.J. Kim³⁸, D.W. Kim³⁷, J.S. Kim³⁷, M. Kim¹²³, S.H. Kim³⁷,
 S. Kim¹⁷, B. Kim¹²³, T. Kim¹²³, S. Kirsch^{36,30}, I. Kisel³⁶, S. Kiselev⁴⁶, A. Kisiel^{30,118}, J.L. Klay⁴,
 J. Klein⁸³, C. Klein-Bösing⁵⁴, M. Kliemant⁵², A. Kluge³⁰, M.L. Knichel⁸⁶, K. Koch⁸³, M.K. Köhler⁸⁶,
 A. Kolojvari¹¹⁷, V. Kondratiev¹¹⁷, N. Kondratyeva⁷⁰, A. Konevskikh⁴⁴, A. Korneev⁸⁸,
 C. Kottachchi Kankanamge Don¹¹⁹, R. Kour⁹¹, M. Kowalski¹⁰⁴, S. Kox⁶⁵, G. Koyithatta Meethalevedu⁴¹,
 J. Kral³⁸, I. Králik⁴⁷, F. Kramer⁵², I. Kraus⁸⁶, T. Krawutschke^{83,31}, M. Kretz³⁶, M. Krivda^{91,47}, F. Krizek³⁸,
 M. Krus³⁴, E. Kryshen⁷⁶, M. Krzewicki^{73,86}, Y. Kucheriaev⁸⁹, C. Kuhn⁵⁸, P.G. Kuijjer⁷³, P. Kurashvili¹⁰¹,
 A.B. Kurepin⁴⁴, A. Kurepin⁴⁴, A. Kuryakin⁸⁸, S. Kushpil⁷⁴, V. Kushpil⁷⁴, H. Kvaerno¹⁸, M.J. Kweon⁸³,
 Y. Kwon¹²³, P. Ladrón de Guevara⁵⁵, I. Lakomov^{42,117}, R. Langoy¹⁵, C. Lara⁵¹, A. Lardeux¹⁰²,
 P. La Rocca²⁴, C. Lazzeroni⁹¹, R. Lea²⁰, Y. Le Bornec⁴², S.C. Lee³⁷, K.S. Lee³⁷, F. Lefèvre¹⁰², J. Lehnert⁵²,
 L. Leistam³⁰, M. Lenhardt¹⁰², V. Lenti⁹⁴, H. León⁵⁶, I. León Monzón¹⁰⁶, H. León Vargas⁵², P. Lévai⁶⁰,
 X. Li¹¹, J. Lien¹⁵, R. Lietava⁹¹, S. Lindal¹⁸, V. Lindenstruth³⁶, C. Lippmann^{86,30}, M.A. Lisa¹⁶, L. Liu¹⁵,
 P.I. Loenne¹⁵, V.R. Loggins¹¹⁹, V. Loginov⁷⁰, S. Lohn³⁰, D. Lohner⁸³, C. Loizides⁶⁸, K.K. Loo³⁸, X. Lopez⁶⁴,
 E. López Torres⁶, G. Løvnhøiden¹⁸, X.-G. Lu⁸³, P. Luettig⁵², M. Lunardon²², J. Luo⁴⁰, G. Luparello⁴⁵,
 L. Luquin¹⁰², C. Luzzi³⁰, R. Ma¹²⁰, K. Ma⁴⁰, D.M. Madagodahettige-Don¹¹⁰, A. Maevskaya⁴⁴,
 M. Mager^{53,30}, D.P. Mahapatra⁴⁸, A. Maire⁵⁸, M. Malaev⁷⁶, I. Maldonado Cervantes⁵⁵, L. Malinina^{59,iii},
 D. Mal'Kevich⁴⁶, P. Malzacher⁸⁶, A. Mamonov⁸⁸, L. Manceau⁹⁵, L. Mangotra⁸¹, V. Manko⁸⁹, F. Manso⁶⁴,
 V. Manzarí⁹⁴, Y. Mao^{65,40}, M. Marchisone^{64,26}, J. Mareš⁴⁹, G.V. Margagliotti^{20,98}, A. Margotti⁹⁶,
 A. Marín⁸⁶, C. Markert¹⁰⁵, I. Martashvili¹¹², P. Martinengo³⁰, M.I. Martínez¹, A. Martínez Davalos⁵⁶,
 G. Martínez García¹⁰², Y. Martynov², A. Mas¹⁰², S. Masciocchi⁸⁶, M. Masera²⁶, A. Masoni⁹³,
 L. Massacrier¹⁰⁹, M. Mastroarco⁹⁴, A. Mastroserio^{28,30}, Z.L. Matthews⁹¹, A. Matyja¹⁰², D. Mayani⁵⁵,
 C. Mayer¹⁰⁴, J. Mazer¹¹², M.A. Mazzoni⁹⁹, F. Meddi²³, A. Menchaca-Rocha⁵⁶, J. Mercado Pérez⁸³,
 M. Meres³³, Y. Miake¹¹⁴, A. Michalon⁵⁸, J. Midori³⁹, L. Milano²⁶, J. Milosevic^{18,iv}, A. Mischke⁴⁵,
 A.N. Mishra⁸², D. Miśkowiec^{86,30}, C. Mitu⁵⁰, J. Mlynarz¹¹⁹, A.K. Mohanty³⁰, B. Mohanty¹¹⁶, L. Molnar³⁰,
 L. Montaña Zetina⁸, M. Monteno⁹⁵, E. Montes⁷, T. Moon¹²³, M. Morando²², D.A. Moreira De Godoy¹⁰⁷,
 S. Moretto²², A. Morsch³⁰, V. Muccifora⁶⁶, E. Mudnic¹⁰³, S. Muhuri¹¹⁶, H. Müller³⁰, M.G. Munhoz¹⁰⁷,
 L. Musa³⁰, A. Musso⁹⁵, B.K. Nandi⁴¹, R. Nania⁹⁶, E. Nappi⁹⁴, C. Nattrass¹¹², N.P. Naumov⁸⁸, S. Navin⁹¹,
 T.K. Nayak¹¹⁶, S. Nazarenko⁸⁸, G. Nazarov⁸⁸, A. Nedosekin⁴⁶, M. Nicassio²⁸, B.S. Nielsen⁷², T. Niida¹¹⁴,
 S. Nikolaev⁸⁹, V. Nikolic⁸⁷, V. Nikulin⁷⁶, S. Nikulin⁸⁹, B.S. Nilsen⁷⁷, M.S. Nilsson¹⁸, F. Noferini^{96,9},
 P. Nomokonov⁵⁹, G. Nooren⁴⁵, N. Novitzky³⁸, A. Nyanin⁸⁹, A. Nyatha⁴¹, C. Nygaard⁷², J. Nystrand¹⁵,
 H. Obayashi³⁹, A. Ochirov¹¹⁷, H. Oeschler^{53,30}, S.K. Oh³⁷, S. Oh¹²⁰, J. Oleniacz¹¹⁸, C. Oppedisano⁹⁵,
 A. Ortiz Velasquez⁵⁵, G. Ortona^{30,26}, A. Oskarsson²⁹, P. Ostrowski¹¹⁸, I. Otterlund²⁹, J. Otwinowski⁸⁶,
 K. Oyama⁸³, K. Ozawa¹¹³, Y. Pachmayer⁸³, M. Pachr³⁴, F. Padilla²⁶, P. Pagano²⁵, G. Paic⁵⁵, F. Painke³⁶,
 C. Pajares¹³, S. Pal¹², S.K. Pal¹¹⁶, A. Palaha⁹¹, A. Palmeri⁹⁷, V. Papikyan¹²¹, G.S. Pappalardo⁹⁷, W.J. Park⁸⁶,
 A. Passfeld⁵⁴, B. Pastirčák⁴⁷, D.I. Patalakha⁴³, V. Paticchio⁹⁴, A. Pavlinov¹¹⁹, T. Pawlak¹¹⁸, T. Peitzmann⁴⁵,
 M. Perales¹⁰, E. Pereira De Oliveira Filho¹⁰⁷, D. Peresunko⁸⁹, C.E. Pérez Lara⁷³, E. Perez Lezama⁵⁵,
 D. Perini³⁰, D. Perrino²⁸, W. Peryt¹¹⁸, A. Pesci⁹⁶, V. Peskov^{30,55}, Y. Pestov³, V. Petráček³⁴, M. Petran³⁴,
 M. Petris⁷¹, P. Petrov⁹¹, M. Petrovici⁷¹, C. Petta²⁴, S. Piano⁹⁸, A. Piccotti⁹⁵, M. Pikna³³, P. Pillot¹⁰²,
 O. Pinazza³⁰, L. Pinsky¹¹⁰, N. Pitz⁵², F. Piuz³⁰, D.B. Piyarathna¹¹⁰, M. Płoskoń⁶⁸, J. Pluta¹¹⁸,
 T. Pocheptsov^{59,18}, S. Pochybova⁶⁰, P.L.M. Podesta-Lerma¹⁰⁶, M.G. Poghosyan^{30,26}, K. Polák⁴⁹,
 B. Polichtchouk⁴³, A. Pop⁷¹, S. Porteboeuf-Houssais⁶⁴, V. Pospíšil³⁴, B. Potukuchi⁸¹, S.K. Prasad¹¹⁹,
 R. Preghenella^{96,9}, F. Prino⁹⁵, C.A. Pruneau¹¹⁹, I. Pshenichnov⁴⁴, S. Puchagin⁸⁸, G. Puudu²¹,
 A. Pulvirenti^{24,30}, V. Punin⁸⁸, M. Putiš³⁵, J. Putschke^{119,120}, E. Quercigh³⁰, H. Qvigstad¹⁸, A. Rachevski⁹⁸,
 A. Rademakers³⁰, S. Radomski⁸³, T.S. Rähö³⁸, J. Rak³⁸, A. Rakotozafindrabe¹², L. Ramello²⁷,
 A. Ramírez Reyes⁸, S. Raniwala⁸², R. Raniwala⁸², S.S. Räsänen³⁸, B.T. Rascanu⁵², D. Rathee⁷⁸,
 K.F. Read¹¹², J.S. Real⁶⁵, K. Redlich^{101,57}, P. Reichelt⁵², M. Reicher⁴⁵, R. Renfordt⁵², A.R. Reolon⁶⁶,
 A. Reshetin⁴⁴, F. Rettig³⁶, J.-P. Revol³⁰, K. Reygers⁸³, L. Riccati⁹⁵, R.A. Ricci⁶⁷, M. Richter¹⁸, P. Riedler³⁰,
 W. Riegler³⁰, F. Riggi^{24,97}, M. Rodríguez Cahuantzi¹, D. Rohr³⁶, D. Röhrich¹⁵, R. Romita⁸⁶, F. Ronchetti⁶⁶,
 P. Rosnet⁶⁴, S. Rosseger³⁰, A. Rossi²², F. Roukoutakis⁷⁹, P. Roy⁹⁰, C. Roy⁵⁸, A.J. Rubio Montero⁷, R. Rui²⁰,

E. Ryabinkin⁸⁹, A. Rybicki¹⁰⁴, S. Sadovsky⁴³, K. Šafařík³⁰, P.K. Sahu⁴⁸, J. Saini¹¹⁶, H. Sakaguchi³⁹, S. Sakai⁶⁸, D. Sakata¹¹⁴, C.A. Salgado¹³, S. Sambyal⁸¹, V. Samsonov⁷⁶, X. Sanchez Castro^{55,58}, L. Šándor⁴⁷, A. Sandoval⁵⁶, M. Sano¹¹⁴, S. Sano¹¹³, R. Santo⁵⁴, R. Santoro^{94,30}, J. Sarkamo³⁸, E. Scapparone⁹⁶, F. Scarlassara²², R.P. Scharenberg⁸⁴, C. Schiaua⁷¹, R. Schicker⁸³, C. Schmidt⁸⁶, H.R. Schmidt^{86,115}, S. Schreiner³⁰, S. Schuchmann⁵², J. Schukraft³⁰, Y. Schutz^{30,102}, K. Schwarz⁸⁶, K. Schweda^{86,83}, G. Scioli¹⁹, E. Scomparin⁹⁵, R. Scott¹¹², P.A. Scott⁹¹, G. Segato²², I. Selyuzhenkov⁸⁶, S. Senyukov^{27,58}, J. Seo⁸⁵, S. Serici²¹, E. Serradilla^{7,56}, A. Sevcenco⁵⁰, I. Sgura⁹⁴, A. Shabetai¹⁰², G. Shabratova⁵⁹, R. Shahoyan³⁰, N. Sharma⁷⁸, S. Sharma⁸¹, K. Shigaki³⁹, M. Shimomura¹¹⁴, K. Shtejer⁶, Y. Sibiriyak⁸⁹, M. Siciliano²⁶, E. Sicking³⁰, S. Siddhanta⁹³, T. Siemiarczuk¹⁰¹, D. Silvermyr⁷⁵, G. Simonetti^{28,30}, R. Singaraju¹¹⁶, R. Singh⁸¹, S. Singha¹¹⁶, B.C. Sinha¹¹⁶, T. Sinha⁹⁰, B. Sitar³³, M. Sitta²⁷, T.B. Skaali¹⁸, K. Skjerdal¹⁵, R. Smakal³⁴, N. Smirnov¹²⁰, R. Snellings⁴⁵, C. Sogaard⁷², R. Soltz⁶⁹, H. Son¹⁷, J. Song⁸⁵, M. Song¹²³, C. Soos³⁰, F. Soramel²², I. Sputowska¹⁰⁴, M. Spyropoulou-Stassinaki⁷⁹, B.K. Srivastava⁸⁴, J. Stachel⁸³, I. Stan⁵⁰, I. Stan⁵⁰, G. Stefanek¹⁰¹, G. Stefanini³⁰, T. Steinbeck³⁶, M. Steinpreis¹⁶, E. Stenlund²⁹, G. Steyn⁸⁰, D. Stocco¹⁰², M. Stolpovskiy⁴³, K. Strabykin⁸⁸, P. Strmen³³, A.A.P. Suaide¹⁰⁷, M.A. Subieta Vázquez²⁶, T. Sugitate³⁹, C. Suire⁴², M. Sukhorukov⁸⁸, R. Sultanov⁴⁶, M. Šumbera⁷⁴, T. Susa⁸⁷, A. Szanto de Toledo¹⁰⁷, I. Szarka³³, A. Szostak¹⁵, C. Tagridis⁷⁹, J. Takahashi¹⁰⁸, J.D. Tapia Takaki⁴², A. Tauro³⁰, G. Tejada Muñoz¹, A. Telesca³⁰, C. Terrevoli²⁸, J. Thäder⁸⁶, J.H. Thomas⁸⁶, D. Thomas⁴⁵, R. Tieulent¹⁰⁹, A.R. Timmins¹¹⁰, D. Tlusty³⁴, A. Toia^{36,30}, H. Torii^{39,113}, L. Toscano⁹⁵, F. Tosello⁹⁵, T. Traczyk¹¹⁸, D. Truesdale¹⁶, W.H. Trzaska³⁸, T. Tsuji¹¹³, A. Tumkin⁸⁸, R. Turrisi¹⁰⁰, T.S. Tveter¹⁸, J. Ulery⁵², K. Ullaland¹⁵, J. Ulrich^{62,51}, A. Uras¹⁰⁹, J. Urbán³⁵, G.M. Urciuoli⁹⁹, G.L. Usai²¹, M. Vajzer^{34,74}, M. Vala^{59,47}, L. Valencia Palomo⁴², S. Vallero⁸³, N. van der Kolk⁷³, P. Vande Vyvre³⁰, M. van Leeuwen⁴⁵, L. Vannucci⁶⁷, A. Vargas¹, R. Varma⁴¹, M. Vasileiou⁷⁹, A. Vasiliev⁸⁹, V. Vechernin¹¹⁷, M. Veldhoen⁴⁵, M. Venaruzzo²⁰, E. Vercellin²⁶, S. Vergara¹, D.C. Verneke⁵⁴, R. Vernet⁵, M. Verweij⁴⁵, L. Vickovic¹⁰³, G. Viesti²², O. Vikhlyantsev⁸⁸, Z. Vilakazi⁸⁰, O. Villalobos Baillie⁹¹, L. Vinogradov¹¹⁷, Y. Vinogradov⁸⁸, A. Vinogradov⁸⁹, T. Virgili²⁵, Y.P. Viyogi¹¹⁶, A. Vodopyanov⁵⁹, S. Voloshin¹¹⁹, K. Voloshin⁴⁶, G. Volpe^{28,30}, B. von Haller³⁰, D. Vranic⁸⁶, G. Øvrebeek¹⁵, J. Vrláková³⁵, B. Vulpescu⁶⁴, A. Vyushin⁸⁸, B. Wagner¹⁵, V. Wagner³⁴, R. Wan^{58,40}, Y. Wang⁸³, M. Wang⁴⁰, D. Wang⁴⁰, Y. Wang⁴⁰, K. Watanabe¹¹⁴, J.P. Wessels^{30,54}, U. Westerhoff⁵⁴, J. Wiechula^{83,115}, J. Wikne¹⁸, M. Wilde⁵⁴, G. Wilk¹⁰¹, A. Wilk⁵⁴, M.C.S. Williams⁹⁶, B. Windelband⁸³, L. Xaplanteris Karampatsos¹⁰⁵, H. Yang¹², S. Yang¹⁵, S. Yano³⁹, S. Yasnopolskiy⁸⁹, J. Yi⁸⁵, Z. Yin⁴⁰, H. Yokoyama¹¹⁴, I.-K. Yoo⁸⁵, J. Yoon¹²³, W. Yu⁵², X. Yuan⁴⁰, I. Yushmanov⁸⁹, C. Zach³⁴, C. Zampolli^{96,30}, S. Zaporozhets⁵⁹, A. Zarochentsev¹¹⁷, P. Závada⁴⁹, N. Zaviyalov⁸⁸, H. Zbroszczyk¹¹⁸, P. Zelnicek^{30,51}, I.S. Zgura⁵⁰, M. Zhalov⁷⁶, X. Zhang^{64,40}, F. Zhou⁴⁰, Y. Zhou⁴⁵, D. Zhou⁴⁰, X. Zhu⁴⁰, A. Zichichi^{19,9}, A. Zimmermann⁸³, G. Zinovjev², Y. Zoccarato¹⁰⁹, M. Zynovyev²

Affiliation notes

- ⁱ Deceased
- ⁱⁱ Also at: Dipartimento di Fisica dell'Università, Udine, Italy
- ⁱⁱⁱ Also at: M.V.Lomonosov Moscow State University, D.V.Skobeltzyn Institute of Nuclear Physics, Moscow, Russia
- ^{iv} Also at: "Vinča" Institute of Nuclear Sciences, Belgrade, Serbia

Collaboration Institutes

- ¹ Benemérita Universidad Autónoma de Puebla, Puebla, Mexico
- ² Bogolyubov Institute for Theoretical Physics, Kiev, Ukraine
- ³ Budker Institute for Nuclear Physics, Novosibirsk, Russia
- ⁴ California Polytechnic State University, San Luis Obispo, California, United States
- ⁵ Centre de Calcul de l'IN2P3, Villeurbanne, France
- ⁶ Centro de Aplicaciones Tecnológicas y Desarrollo Nuclear (CEADEN), Havana, Cuba
- ⁷ Centro de Investigaciones Energéticas Medioambientales y Tecnológicas (CIEMAT), Madrid, Spain
- ⁸ Centro de Investigación y de Estudios Avanzados (CINVESTAV), Mexico City and Mérida, Mexico
- ⁹ Centro Fermi – Centro Studi e Ricerche e Museo Storico della Fisica "Enrico Fermi", Rome, Italy
- ¹⁰ Chicago State University, Chicago, United States
- ¹¹ China Institute of Atomic Energy, Beijing, China
- ¹² Commissariat à l'Énergie Atomique, IRFU, Saclay, France

- 13 Departamento de Física de Partículas and IGFAE, Universidad de Santiago de Compostela, Santiago de Compostela, Spain
- 14 Department of Physics Aligarh Muslim University, Aligarh, India
- 15 Department of Physics and Technology, University of Bergen, Bergen, Norway
- 16 Department of Physics, Ohio State University, Columbus, Ohio, United States
- 17 Department of Physics, Sejong University, Seoul, South Korea
- 18 Department of Physics, University of Oslo, Oslo, Norway
- 19 Dipartimento di Fisica dell'Università and Sezione INFN, Bologna, Italy
- 20 Dipartimento di Fisica dell'Università and Sezione INFN, Trieste, Italy
- 21 Dipartimento di Fisica dell'Università and Sezione INFN, Cagliari, Italy
- 22 Dipartimento di Fisica dell'Università and Sezione INFN, Padova, Italy
- 23 Dipartimento di Fisica dell'Università 'La Sapienza' and Sezione INFN, Rome, Italy
- 24 Dipartimento di Fisica e Astronomia dell'Università and Sezione INFN, Catania, Italy
- 25 Dipartimento di Fisica 'E.R. Caianiello' dell'Università and Gruppo Collegato INFN, Salerno, Italy
- 26 Dipartimento di Fisica Sperimentale dell'Università and Sezione INFN, Turin, Italy
- 27 Dipartimento di Scienze e Tecnologie Avanzate dell'Università del Piemonte Orientale and Gruppo Collegato INFN, Alessandria, Italy
- 28 Dipartimento Interateneo di Fisica 'M. Merlin' and Sezione INFN, Bari, Italy
- 29 Division of Experimental High Energy Physics, University of Lund, Lund, Sweden
- 30 European Organization for Nuclear Research (CERN), Geneva, Switzerland
- 31 Fachhochschule Köln, Köln, Germany
- 32 Faculty of Engineering, Bergen University College, Bergen, Norway
- 33 Faculty of Mathematics, Physics and Informatics, Comenius University, Bratislava, Slovakia
- 34 Faculty of Nuclear Sciences and Physical Engineering, Czech Technical University in Prague, Prague, Czech Republic
- 35 Faculty of Science, P.J. Šafárik University, Košice, Slovakia
- 36 Frankfurt Institute for Advanced Studies, Johann Wolfgang Goethe-Universität Frankfurt, Frankfurt, Germany
- 37 Gangneung-Wonju National University, Gangneung, South Korea
- 38 Helsinki Institute of Physics (HIP) and University of Jyväskylä, Jyväskylä, Finland
- 39 Hiroshima University, Hiroshima, Japan
- 40 Hua-Zhong Normal University, Wuhan, China
- 41 Indian Institute of Technology, Mumbai, India
- 42 Institut de Physique Nucléaire d'Orsay (IPNO), Université Paris-Sud, CNRS-IN2P3, Orsay, France
- 43 Institute for High Energy Physics, Protvino, Russia
- 44 Institute for Nuclear Research, Academy of Sciences, Moscow, Russia
- 45 Nikhef, National Institute for Subatomic Physics and Institute for Subatomic Physics of Utrecht University, Utrecht, Netherlands
- 46 Institute for Theoretical and Experimental Physics, Moscow, Russia
- 47 Institute of Experimental Physics, Slovak Academy of Sciences, Košice, Slovakia
- 48 Institute of Physics, Bhubaneswar, India
- 49 Institute of Physics, Academy of Sciences of the Czech Republic, Prague, Czech Republic
- 50 Institute of Space Sciences (ISS), Bucharest, Romania
- 51 Institut für Informatik, Johann Wolfgang Goethe-Universität Frankfurt, Frankfurt, Germany
- 52 Institut für Kernphysik, Johann Wolfgang Goethe-Universität Frankfurt, Frankfurt, Germany
- 53 Institut für Kernphysik, Technische Universität Darmstadt, Darmstadt, Germany
- 54 Institut für Kernphysik, Westfälische Wilhelms-Universität Münster, Münster, Germany
- 55 Instituto de Ciencias Nucleares, Universidad Nacional Autónoma de México, Mexico City, Mexico
- 56 Instituto de Física, Universidad Nacional Autónoma de México, Mexico City, Mexico
- 57 Institut of Theoretical Physics, University of Wrocław
- 58 Institut Pluridisciplinaire Hubert Curien (IPHC), Université de Strasbourg, CNRS-IN2P3, Strasbourg, France
- 59 Joint Institute for Nuclear Research (JINR), Dubna, Russia
- 60 KFKI Research Institute for Particle and Nuclear Physics, Hungarian Academy of Sciences, Budapest, Hungary
- 61 Kharkiv Institute of Physics and Technology (KIPT), National Academy of Sciences of Ukraine (NASU),

- Kharkov, Ukraine
- 62 Kirchhoff-Institut für Physik, Ruprecht-Karls-Universität Heidelberg, Heidelberg, Germany
- 63 Korea Institute of Science and Technology Information
- 64 Laboratoire de Physique Corpusculaire (LPC), Clermont Université, Université Blaise Pascal, CNRS-IN2P3, Clermont-Ferrand, France
- 65 Laboratoire de Physique Subatomique et de Cosmologie (LPSC), Université Joseph Fourier, CNRS-IN2P3, Institut Polytechnique de Grenoble, Grenoble, France
- 66 Laboratori Nazionali di Frascati, INFN, Frascati, Italy
- 67 Laboratori Nazionali di Legnaro, INFN, Legnaro, Italy
- 68 Lawrence Berkeley National Laboratory, Berkeley, California, United States
- 69 Lawrence Livermore National Laboratory, Livermore, California, United States
- 70 Moscow Engineering Physics Institute, Moscow, Russia
- 71 National Institute for Physics and Nuclear Engineering, Bucharest, Romania
- 72 Niels Bohr Institute, University of Copenhagen, Copenhagen, Denmark
- 73 Nikhef, National Institute for Subatomic Physics, Amsterdam, Netherlands
- 74 Nuclear Physics Institute, Academy of Sciences of the Czech Republic, Řež u Prahy, Czech Republic
- 75 Oak Ridge National Laboratory, Oak Ridge, Tennessee, United States
- 76 Petersburg Nuclear Physics Institute, Gatchina, Russia
- 77 Physics Department, Creighton University, Omaha, Nebraska, United States
- 78 Physics Department, Panjab University, Chandigarh, India
- 79 Physics Department, University of Athens, Athens, Greece
- 80 Physics Department, University of Cape Town, iThemba LABS, Cape Town, South Africa
- 81 Physics Department, University of Jammu, Jammu, India
- 82 Physics Department, University of Rajasthan, Jaipur, India
- 83 Physikalisches Institut, Ruprecht-Karls-Universität Heidelberg, Heidelberg, Germany
- 84 Purdue University, West Lafayette, Indiana, United States
- 85 Pusan National University, Pusan, South Korea
- 86 Research Division and ExtreMe Matter Institute EMMI, GSI Helmholtzzentrum für Schwerionenforschung, Darmstadt, Germany
- 87 Rudjer Bošković Institute, Zagreb, Croatia
- 88 Russian Federal Nuclear Center (VNIIEF), Sarov, Russia
- 89 Russian Research Centre Kurchatov Institute, Moscow, Russia
- 90 Saha Institute of Nuclear Physics, Kolkata, India
- 91 School of Physics and Astronomy, University of Birmingham, Birmingham, United Kingdom
- 92 Sección Física, Departamento de Ciencias, Pontificia Universidad Católica del Perú, Lima, Peru
- 93 Sezione INFN, Cagliari, Italy
- 94 Sezione INFN, Bari, Italy
- 95 Sezione INFN, Turin, Italy
- 96 Sezione INFN, Bologna, Italy
- 97 Sezione INFN, Catania, Italy
- 98 Sezione INFN, Trieste, Italy
- 99 Sezione INFN, Rome, Italy
- 100 Sezione INFN, Padova, Italy
- 101 Soltan Institute for Nuclear Studies, Warsaw, Poland
- 102 SUBATECH, Ecole des Mines de Nantes, Université de Nantes, CNRS-IN2P3, Nantes, France
- 103 Technical University of Split FESB, Split, Croatia
- 104 The Henryk Niewodniczanski Institute of Nuclear Physics, Polish Academy of Sciences, Cracow, Poland
- 105 The University of Texas at Austin, Physics Department, Austin, TX, United States
- 106 Universidad Autónoma de Sinaloa, Culiacán, Mexico
- 107 Universidade de São Paulo (USP), São Paulo, Brazil
- 108 Universidade Estadual de Campinas (UNICAMP), Campinas, Brazil
- 109 Université de Lyon, Université Lyon 1, CNRS/IN2P3, IPN-Lyon, Villeurbanne, France
- 110 University of Houston, Houston, Texas, United States
- 111 University of Technology and Austrian Academy of Sciences, Vienna, Austria
- 112 University of Tennessee, Knoxville, Tennessee, United States
- 113 University of Tokyo, Tokyo, Japan

- ¹¹⁴ University of Tsukuba, Tsukuba, Japan
- ¹¹⁵ Eberhard Karls Universität Tübingen, Tübingen, Germany
- ¹¹⁶ Variable Energy Cyclotron Centre, Kolkata, India
- ¹¹⁷ V. Fock Institute for Physics, St. Petersburg State University, St. Petersburg, Russia
- ¹¹⁸ Warsaw University of Technology, Warsaw, Poland
- ¹¹⁹ Wayne State University, Detroit, Michigan, United States
- ¹²⁰ Yale University, New Haven, Connecticut, United States
- ¹²¹ Yerevan Physics Institute, Yerevan, Armenia
- ¹²² Yildiz Technical University, Istanbul, Turkey
- ¹²³ Yonsei University, Seoul, South Korea
- ¹²⁴ Zentrum für Technologietransfer und Telekommunikation (ZTT), Fachhochschule Worms, Worms, Germany